

RESEARCH ARTICLE

10.1002/2013WR014451

Key Points:

- Numerical groundwater model of folded and faulted intermountain basin
- Different landscapes form topography or permeability controlled flow systems
- Geologic structure controls recharge mechanisms in valley aquifers

Correspondence to:

L. B. Ball,
lball@usgs.gov

Citation:

Ball, L. B., J. S. Caine, and S. Ge (2014), Controls on groundwater flow in a semiarid folded and faulted intermountain basin, *Water Resour. Res.*, 50, doi:10.1002/2013WR014451.

Received 19 JUL 2013

Accepted 23 JUL 2014

Accepted article online 25 JUL 2014

Controls on groundwater flow in a semiarid folded and faulted intermountain basin

Lyndsay B. Ball¹, Jonathan Saul Caine¹, and Shemin Ge²

¹U.S. Geological Survey, Denver, Colorado, USA, ²Department of Geological Sciences, University of Colorado, Boulder, Colorado, USA

Abstract The major processes controlling groundwater flow in intermountain basins are poorly understood, particularly in basins underlain by folded and faulted bedrock and under regionally realistic hydrogeologic heterogeneity. To explore the role of hydrogeologic heterogeneity and poorly constrained mountain hydrologic conditions on regional groundwater flow in contracted intermountain basins, a series of 3-D numerical groundwater flow models were developed using the South Park basin, Colorado, USA as a proxy. The models were used to identify the relative importance of different recharge processes to major aquifers, to estimate typical groundwater circulation depths, and to explore hydrogeologic communication between mountain and valley hydrogeologic landscapes. Modeling results show that mountain landscapes develop topographically controlled and predominantly local-scale to intermediate-scale flow systems. Permeability heterogeneity of the fold and fault belt and decreased topographic roughness led to permeability controlled flow systems in the valley. The structural position of major aquifers in the valley fold and fault belt was found to control the relative importance of different recharge mechanisms. Alternative mountain recharge model scenarios showed that higher mountain recharge rates led to higher mountain water table elevations and increasingly prominent local flow systems, primarily resulting in increased seepage within the mountain landscape and nonlinear increases in mountain block recharge to the valley. Valley aquifers were found to be relatively insensitive to changing mountain water tables, particularly in structurally isolated aquifers inside the fold and fault belt.

1. Introduction

Expanding population centers are placing increasing demand on limited water supplies in arid and semiarid regions, particularly in the western United States. As surface water is already heavily allocated in most western rivers, groundwater resources in intermountain basins are increasingly being sought to meet these growing demands. The broad valleys between adjacent mountain ranges are appealing targets to supplement water supplies [e.g., Marler and Ge, 2003; Zektser et al., 2005; Gillespie et al., 2012]. In arid and semiarid environments, valley aquifers are likely to be dependent upon mountain precipitation for recharge. Recharge primarily occurs through losing streams draining the adjacent mountains or from mountain block recharge (MBR) below the mountain-valley landscape interface [Wilson and Guan, 2004; Manning and Solomon, 2005; Gleeson and Manning, 2008]. However, the major processes governing flow between mountain recharge locations and valley aquifers are poorly understood, particularly under realistically heterogeneous hydrogeologic conditions. To effectively monitor the groundwater resources of intermountain basins and predict the impact of stresses presented by new water resource development or changing climatic conditions, the factors that control basin-wide groundwater flow and groundwater interaction between mountain-valley landscapes need to be better understood.

Prior study of groundwater systems in mountainous terrain has largely been based on schematic models that simplify hydrogeologic heterogeneity, including linear stream networks, smooth topographic slopes, and homogeneous aquifers or those with horizontally layered geology. Such schematic models have led to insights into the relations among bulk permeability, recharge rates, and simple topographic incision that define the present-day conceptualization of how mountain water tables are configured and controlled [e.g., Toth, 1963; Forster and Smith, 1988a, 1988b; Haitjema and Mitchell-Bruker, 2005; Gleeson and Manning, 2008; Jiang et al., 2009]. Welch and Allen [2012] have recently expanded on this work and found the concepts from the schematic models to be valid in topographically realistic numerical flow models of relatively small

mountain watersheds. These various model results in combination with environmental tracer analysis [Manning and Soloman, 2005; Manning, 2011] suggest that MBR makes substantial contributions to valley aquifers. However, the role that realistic heterogeneity plays in basin-scale groundwater flow and MBR to valley aquifers is not addressed by these prior studies. Previous studies also commonly treat the mountain-valley interface as a boundary condition, and the fate of MBR within valley aquifers is not simulated.

Intermountain basins are unique relative to other groundwater flow systems in part because of the characteristic degree of heterogeneity. Such heterogeneity includes large topographic relief, substantial climatic differences over small distances, and variable permeability structure due to lithological and geological complexities formed by tectonic activity. These heterogeneities can lead to unique and highly dynamic groundwater flow systems. The high topography of mountains can cause steep hydraulic gradients and potentially deep groundwater circulation [Toth, 1963]. Changes in climatic variables that come with variations in elevation, aspect, and orographically controlled precipitation patterns can result in highly variable recharge patterns. Bedrock aquifers and aquitards are commonly fractured, faulted, and folded, resulting in variable geometry and hydraulic properties that can have substantial impact to groundwater flow [Forster and Smith, 1988a; Lopez and Smith, 1995, 1996]. Our limited ability to characterize hydrogeologic heterogeneity and a lack of high elevation wells to adequately describe the hydrogeologic conditions in the high-elevation terrains of intermountain basins makes development of conceptual and numerical models particularly challenging and useful for understanding of the basic patterns and dynamics of groundwater flow.

Numerical groundwater modeling studies of intermountain basins have previously focused on fault-block-style extensional basins containing relatively uniform unconsolidated or poorly lithified aquifers in the valleys [e.g., Keating *et al.*, 2003; Sanford *et al.*, 2004]. Basins formed from contractional tectonic processes, in contrast, also are common geologic settings (e.g., Snyderville basin, Utah [Susong *et al.*, 1998]; Ebro basin, Spain [Carceller-Layel *et al.*, 2007]; Denver basin, Colorado [Belitz and Bredehoeft, 1988]). These basins have broad valleys surrounded by mountains and are underlain by rocks that have been folded and faulted by past contractional deformation, leading to a characteristic hydrogeologic setting defined by: (1) complex landforms including nonlinear valley shapes and geologically controlled stream drainage networks, (2) geologic formations with a range of rock types and hydraulic properties that have been folded, resulting in interlayered aquifers and aquitards with variable dip angles and structural positions, and (3) large displacement faults that can juxtapose aquifers against aquitards and introduce their own distinct fault zone architecture and permeability structure. These heterogeneities present unique challenges to developing regional scale conceptual and numerical models, and the approach taken here provides an example of model development for these complex regions.

This study presents a series of regional-scale numerical groundwater flow models of a semiarid intermountain basin where the underlying geology is characterized by contractional deformation of sedimentary rocks, the South Park basin in central Colorado, USA. The models use the actual basin topography and a regional conceptualization of a realistic fold-fault belt permeability structure. As such, the modeling results presented here honor the realistic, regional-scale heterogeneity of South Park as a proxy for intermountain basins underlain by complex geology. A series of different mountain recharge rates were used to develop six models representing a variety of hydrogeologic conditions realistic for semiarid mountainous regions. The models are used to assess the role of permeability and topographic heterogeneity on controlling regional groundwater flow and mountain-valley groundwater interaction, to explore the relative importance of mountain water table elevations in basin-wide groundwater flow, and to evaluate how changing recharge rates in the mountain block may impact the valley aquifer systems. We simulate groundwater flow throughout the entire intermountain basin, allowing full interaction between mountain and valley aquifers and enabling interpretation of the fate of MBR in valley aquifers, particularly with respect to the understudied impact of fold-fault belt geology on groundwater flow.

2. Description of Study Area

South Park is a large (>3300 km²), semiarid intermountain basin with an expansive, high altitude valley (2600–3000 m elevation) between the Front and Mosquito Ranges (Figure 1). The majority of the main valley is open grassland surrounded by forested mountainous terrain. The South Park basin is sparsely populated, where fewer than 8000 residents are estimated to live in a few small towns and several low-density

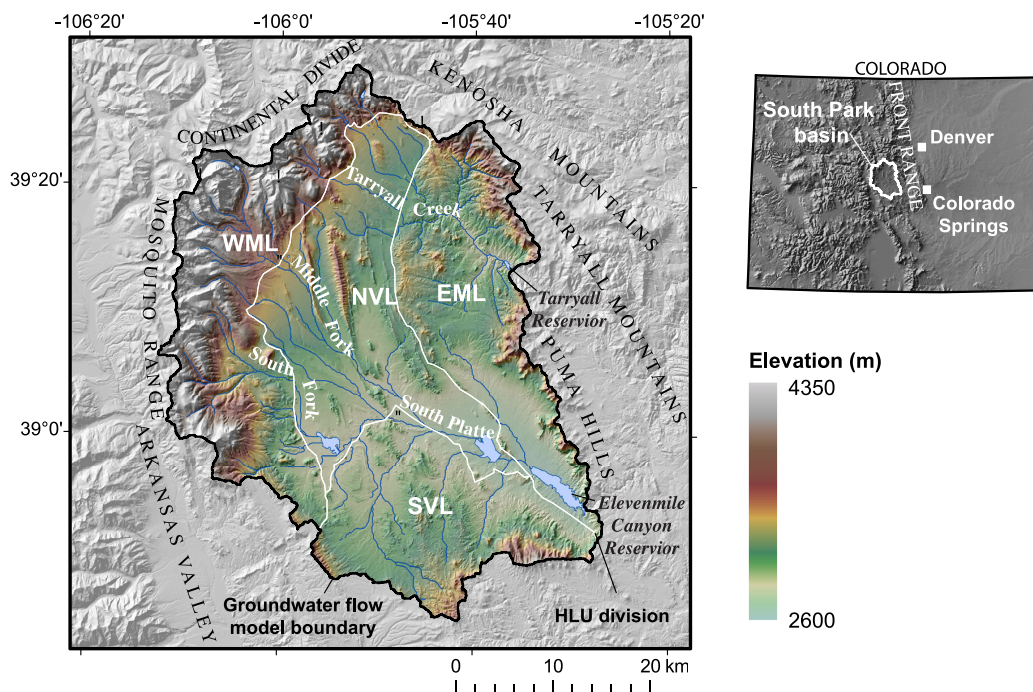


Figure 1. Site map showing the major topographic and hydrologic features of the South Park basin in central Colorado, USA. Hydrogeologic landscape units (HLUs) used in model conceptualization are shown as white lines and include western mountain landscape, WML; northern valley landscape, NVL; eastern mountain landscape, EML; and southern volcanic landscape, SVL.

residential developments. However, the basin is within 60 km of the expanding Front Range suburban corridor between Denver and Colorado Springs (Figure 1), where population estimates exceeded 3 million residents in the 2010 U.S. Census. South Park forms a large catchment area for the headwaters of the South Platte River, one of the primary water sources for the greater Denver metropolitan area and agricultural communities of Colorado’s eastern plains. Surface water has historically dominated the Front Range water supply, but existing stream flows are heavily allocated to senior water users and groundwater is becoming an increasingly sought-after resource [Topper *et al.*, 2003].

The hydrogeology of the South Park basin has not been studied at the basin-wide scale and the regional dynamics and patterns of the groundwater flow system remain uncharacterized. Subbasin scale studies have included the seasonality of groundwater levels and fluctuations in water quality in the northeast portion of the valley [Bruce and Kimbrough, 1999], estimates of potential evapotranspiration (ET) at a few locations [Spahr, 1981], the study of fault permeability at one location [Ball *et al.*, 2010; Marler and Ge, 2003], and several local investigations of calcareous fens [Chapman *et al.*, 2003; Cooper, 1996; Johnson and Stiengraeber, 2003; Legg, 2011].

The South Park basin is delineated by topographic drainage divides encompassing a 3360 km² area. The northwestern divide of the basin coincides with the Continental Divide (Figure 1). The western divide is the crest of the Mosquito Range and separates the South Platte and Arkansas River basins. The eastern divide marks the western edge of the Front Range Mountains and is locally defined by the Tarryall and Kenosha Mountains and the Puma Hills. The South Platte River and its tributary, Tarryall Creek, flow through incised valleys at the eastern boundary. The southern divide is the least topographically pronounced and is geomorphically influenced by the adjacent high country of the Thirty-nine Mile volcanic field.

2.1. Hydrogeologic Landscapes of the South Park Basin

An intermountain basin can contain a variety of distinct hydrogeologic landscapes consisting of mountain and valley regions, each of which is likely to have distinct groundwater flow dynamics [Winter, 2001]. We conceptualize South Park with four major hydrogeologic landscape units (HLU): the Western Mountain Landscape (WML), Northern Valley Landscape (NVL), Southern Volcanic Landscape (SVL), and Eastern

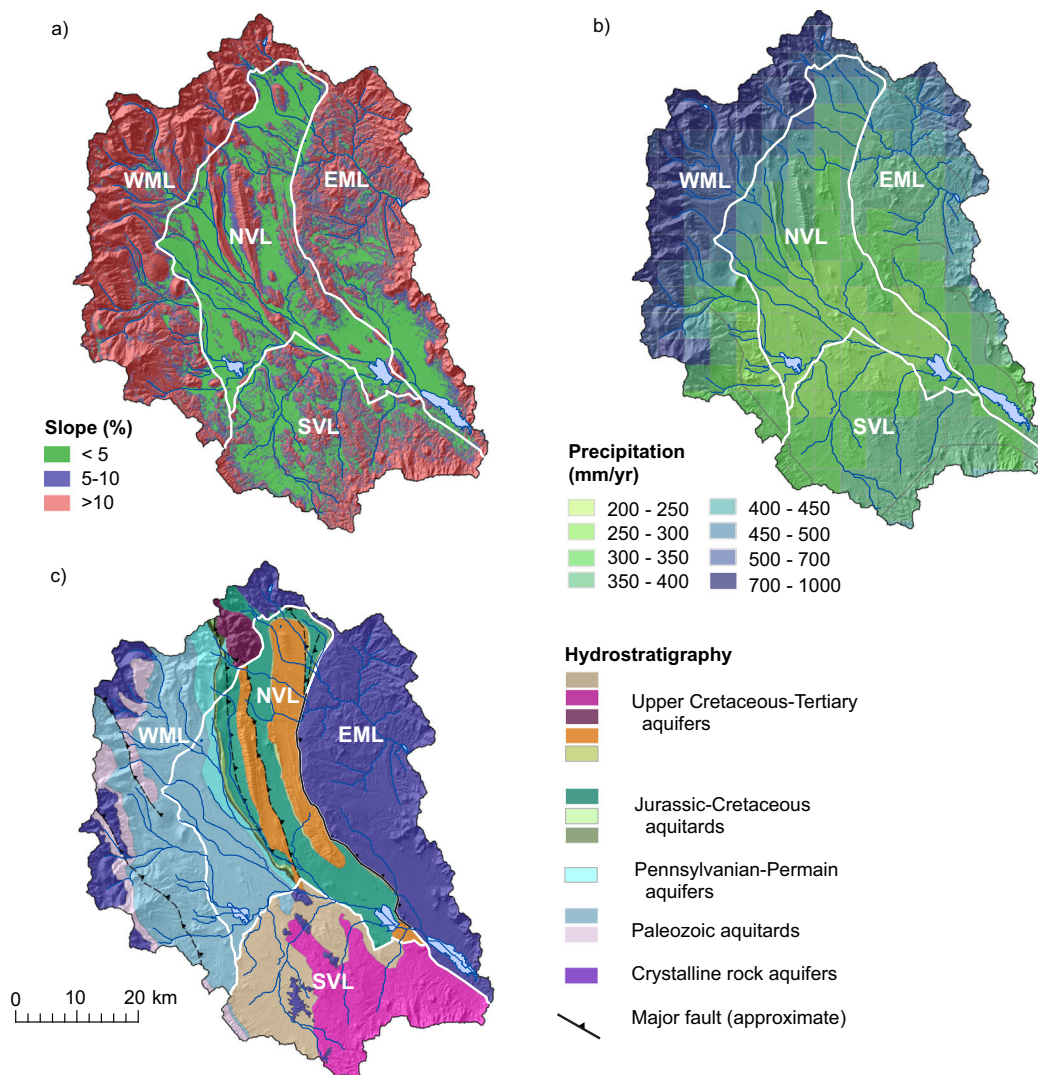


Figure 2. Maps showing primary features used to define the hydrogeologic landscape units of the South Park basin: (a) topographic landforms derived from the 30 m USGS National Elevation Data Set; (b) climatic variability derived from Parameter-Elevation Regressions on Independent Slopes Model (PRISM) mean annual precipitation models, 1970–2000, and (c) regional-scale surface bedrock geology. Detailed hydrostratigraphic descriptions are given in Figure 3. (Western mountain landscape, WML; northern valley landscape, NVL; eastern mountain landscape, EML; and southern volcanic landscape, SVL.)

Mountain Landscape (EML; Figure 1). These landscapes were chosen for their characteristic topography, climate, and geology and were used in the conceptual development of the numerical flow model (Figure 2).

The WML extends from the crest of the Mosquito Range to the major break in slope, which marks the boundary with the relatively flat NVL (Figures 1 and 2a). Steep slopes and deeply incised drainages characterize the WML. Precipitation ranges from <400 in lower elevation areas to >700 mm/yr in the highest terrain, the majority of which falls as snow during the winter and spring months (Figure 2b; Natural Resource Conservation Service (NRCS) Snow Telemetry (SNOTEL) data, <http://www.wcc.nrcs.usda.gov/snotel/Colorado/colorado.html>). Mean winter and summer temperatures range between –10 and 14°C for monitoring sites between 3150 and 3500 m elevation (SNOTEL data, four stations). Stream hydrographs indicate perennial stream flow to at least an elevation of 3150 m based on gage locations (U.S. Geological Survey (USGS) National Water Information System (NWIS) data, <http://waterdata.usgs.gov/nwis/gw>). Low flows occur between January and March and peak flows occur in June when snowmelt is at its highest. The geology of the WML consists of up to 3.5 km thick Paleozoic and Mesozoic carbonate and clastic sedimentary rocks unconformably overlying Proterozoic crystalline basement rocks (Figure 2c) [Ball, 2012, and references

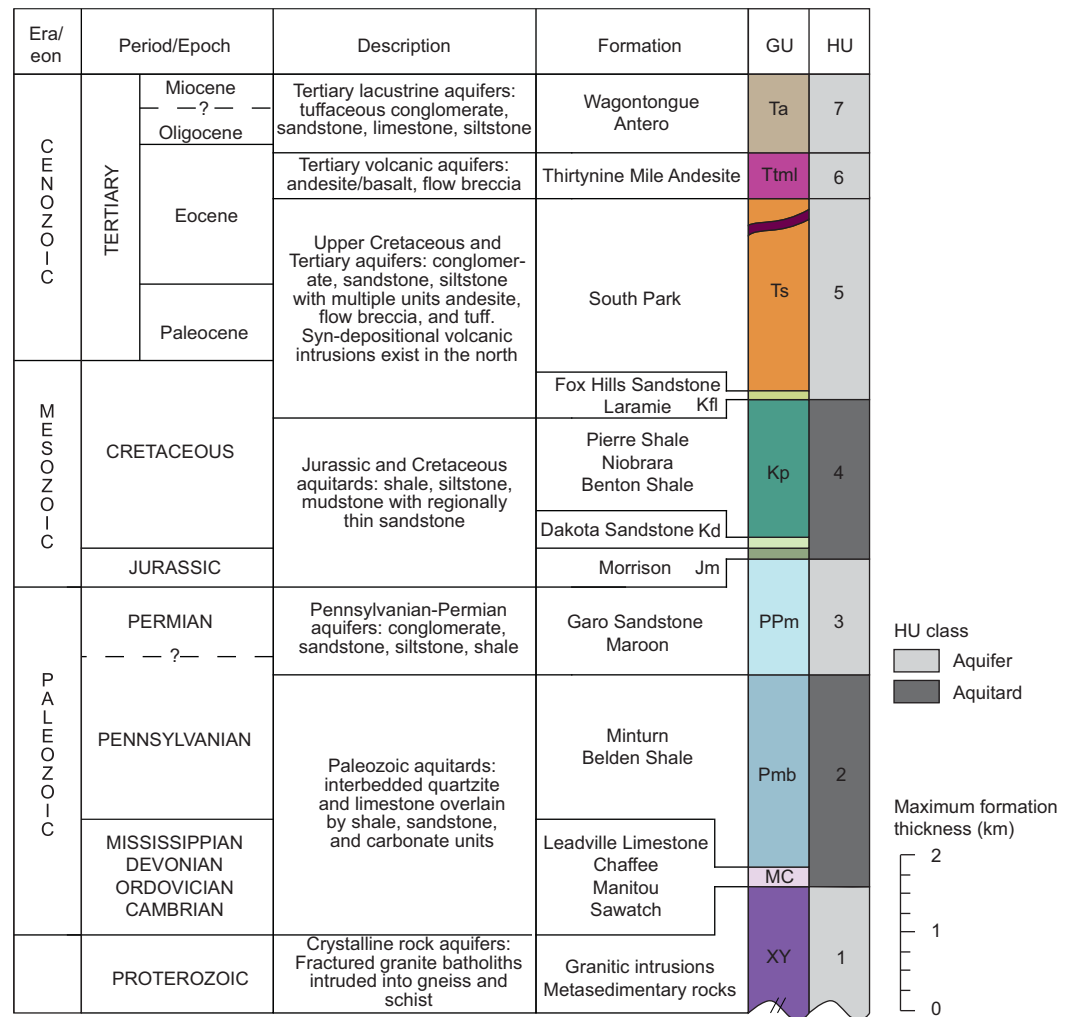


Figure 3. Stratigraphic column describing the regional geologic map units (GU) of the South Park basin and their conceptualization into hydrostratigraphic units (HU).

therein]. Tertiary igneous intrusions can be found throughout the WML and range in size from small sills and dikes to large batholiths (~1.3% of basin-wide land surface area). Land cover includes bare rock and soil, grasses, shrubs, and forest common to alpine and subalpine regions.

The NVL is a topographically flat area relative to the surrounding mountainous terrain and composes the majority of South Park’s valley (Figures 1 and 2a). The geology of this landscape is dominated by a contractional fold-and-fault belt consisting of Paleozoic, Mesozoic, and Cenozoic sedimentary rocks with multiple volcanic layers (Figure 2b). The total thickness of the sedimentary sequence varies and likely exceeds 5 km at its thickest in the north-central part of the NVL [Ball, 2012, and references therein]. Erosionally resistant formations form strike ridges that interrupt this otherwise low-relief landscape. Meteorological observations are limited for the NVL, but the available record suggests that the valley receives less than half the precipitation of the WML, primarily from summer convective storm events (SNOTEL data). Snow accumulation in the northern valley tends to drift by wind transport, and infiltration is likely to be spatially variable. Mean monthly temperatures generally range between -8 and 17°C for the winter and summer, respectively (SNOTEL data). The NVL contains two major streams separated by a subtle topographic rise (Figure 1): the South Platte River in the south, including its major tributaries of the Middle and South Forks, and Tarryall Creek in the north. Tarryall Creek joins the South Platte River about 18 km downstream of Elevenmile Canyon Reservoir (Figure 1). The vegetation of the NVL is dominated by shortgrass prairie, although small conifers and aspen stands are present along north-facing ridges. Several alkaline fens exist in the NVL, and major ion chemistry suggests they act as groundwater discharge locations [Chapman et al., 2003].

The SVL is similar in climate to the NVL, but the bedrock geology is overlain by Tertiary volcanic rocks that compose the northern portion of the Thirtynine Mile volcanic field (Figure 2b). Tuffaceous lake sediments, volcanic flows, and tuffs blanket the majority of this region. These formations lead to surface topography that is generally more rolling than that of the NVL, and the valley gradually rises in elevation toward the southern basin divide separating the South Platte and Arkansas River watersheds (Figure 1). The prevolcanic geology of the SVL is poorly exposed with the exception of some outcrops of Proterozoic granites, suggesting that the folded and faulted sedimentary rocks that dominate the geology in the NVL become thinner to absent in the SVL, and that the crystalline basement is substantially shallower.

The EML has lower topographic relief than the WML, but is generally higher in elevation than the SVL or NVL. The boundary between the valley landscapes and the EML is defined by the western edge of exposed Proterozoic crystalline rocks believed to compose the hanging wall of the Elkhorn fault. The Elkhorn is a Laramide-aged, east-dipping reverse fault that likely accommodates several kilometers of displacement and juxtaposes crystalline rocks with sedimentary strata in much of the central part of the basin [Bryant *et al.*, 1981; Ruleman *et al.*, 2011; Sterne, 2006]. This crystalline/sedimentary contact extends to the north beyond the mapped fault trace, where Cretaceous and sedimentary rocks are likely to lie in depositional unconformity on the crystalline rocks. Stream gages indicate perennial conditions (NWIS data). The area is generally vegetated by conifers and aspens, although the southern extent of the EML is covered in shortgrass prairie.

3. Numerical Groundwater Flow Models

A series of saturated steady state numerical groundwater flow models were constructed for the South Park basin to represent a “best fit” reference model that reasonably recreates available field observations and five additional models simulating a range of recharge conditions in the WML. All models were created using the Finite-Element Subsurface Flow and Transport Simulation System (FEFLOW; (DHI-WASY GmbH, Berlin, Germany)). Processes occurring in the unsaturated zone, such as interflow to streams or changes in soil moisture, are not directly simulated. By assuming steady state conditions, groundwater flow was examined under long-term equilibrium conditions. The water table configuration is assumed to remain relatively similar throughout the year and seasonal variations are not expected to have a substantial impact on basin-scale groundwater flow patterns. Available monthly water-level data support this assumption and indicate seasonal water table variations in valley aquifers of 2–4 m. This variability is negligible given that the range in water table elevation is expected to exceed 1 km between the mountain and valley landscapes.

The model perimeter coincides with the major topographic divides defining the regional surface watershed of the South Park basin (Figure 1). The USGS 30 m resolution National Elevation Dataset (NED30) was used to define the land surface topography for all georeferenced supporting data, including hydrostratigraphy, stream locations, and field observation data. The total depth of the model was extended 6 km below the land surface to allow for deep circulation and to capture the full thickness of the hydrostratigraphy (Figures 3 and 4). The model domain was discretized into 2.4 million triangular, prismatic elements configured in 10 layers. Layers generally increase in thickness with depth: layers 1–5 are 100 m thick, layer 6 is 500 m, layers 7–9 are 1000 m, and layer 10 is 2000 m. The triangular elements range in width from about 500 to <50 m near assigned boundary conditions, hydraulic head observation points used in model performance assessment, or locations in the model where smaller spatial steps improved computational efficiency.

3.1. Boundary Conditions

3.1.1. Model Perimeter Boundary Conditions

The geographic extent of the model domain was selected to allow for clear boundary condition assignments at the model perimeter. The major topographic divides defining the model domain were assumed to behave as groundwater divides and were represented by no-flow boundary conditions over the majority of the model perimeter. Tarryall and Elevenmile Canyon Reservoirs provided reasonable constraints on the hydraulic head at the regional outlets at the eastern model perimeter (Figure 1). The water-surface elevation of both reservoirs was used to define constant-head boundary conditions for the full vertical extent of the model perimeter coinciding with the each reservoir.

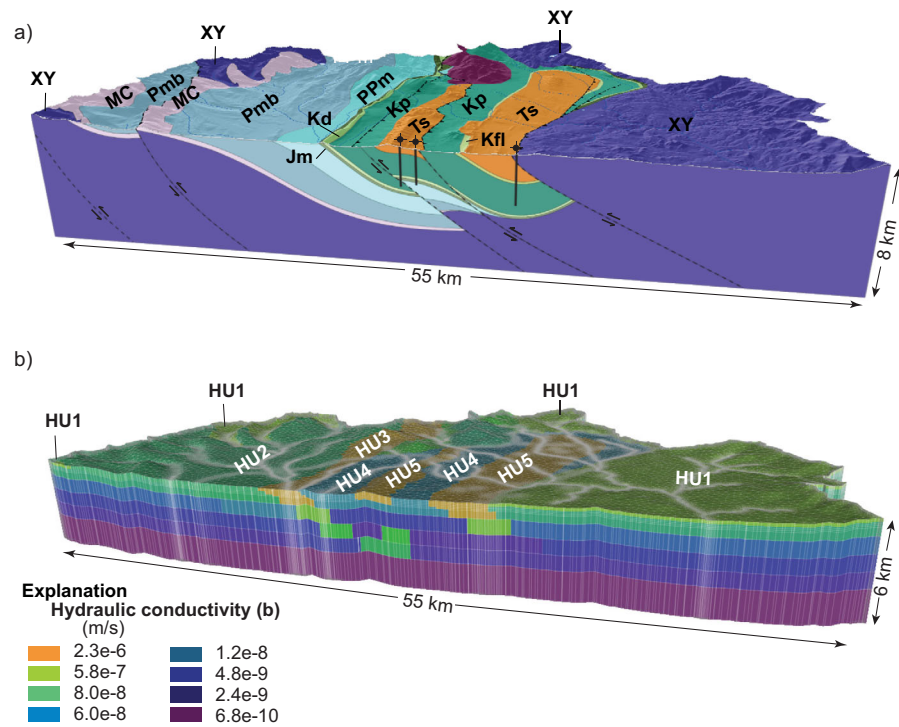


Figure 4. Three-dimensional models showing an example of the translation of (a) regional bedrock geology to (b) the hydraulic conductivity structure of the numerical groundwater flow model. Geologic units are defined in Figure 3, along with the correlation to hydrostratigraphic units (HU) used to define the hydraulic conductivity of the groundwater flow model.

3.1.2. Upper Surface Boundary Conditions

The water table acts as the upper boundary of the model domain and was treated as a free surface with a moveable mesh. The top of the upper layer coincides with the simulated water table instead of the land surface, ensuring that all elements are saturated over their full height. The movable mesh allows the layer elevations to change between model iterations as the water table is recalculated, with an upper threshold elevation defined as the reference elevation of the land surface. This was implemented using the Best-Adaptation-to-Stratigraphic-Data technique in FEFLOW [Diersch, 1998], which allows the element geometry to shift while minimizing changes to the initially assigned hydrostratigraphy.

Areal groundwater recharge (AR), the fluid flux reaching the water table through infiltration of precipitation, and (or) snowmelt, was simulated on the basis of regionalized precipitation distribution. Distributed mean annual precipitation data were taken from 1970 to 2000 averages calculated by the 4 km resolution Parameter-Elevation Regressions on Independent Slopes Model (PRISM) [Daly et al., 2002; PRISM Climate Group, 2006] (Figure 2b). The average annual precipitation rate of each HLU (P_{HLU}) was estimated by redistributing the estimated annual precipitation for individual PRISM cells (P_c) using the following summation:

$$P_{HLU} = \frac{\sum_{c=1}^n P_c a_c}{A_{HLU}} \quad (1)$$

where a_c is the area of the individual PRISM cell, n is the total number of cells in a given HLU, and A_{HLU} is the total area of the HLU. PRISM cells along HLU boundaries were split along the boundary to preserve the HLU area.

AR rates were estimated as a ratio of AR to P_{HLU} (AR/P) using guidance from studies in similar semiarid and mountainous watersheds. Previous studies in Colorado mountain landscapes suggest AR/P between 0.14 and 0.18 [Huntley, 1979; Bossong et al., 2003]. In addition to these local estimates, AR/P for other semiarid and mountainous basins have been reported to vary between 0.03 and 0.42 AR/P with a median value of 0.15 ($n = 14$) [Scanlon et al., 2006; Wilson and Guan, 2004]. Various combinations of AR/P within this range

were explored during the model performance evaluation process (described in section 3.2), and final AR rates for the reference model were selected to optimize the model's simulation of observed field conditions.

Because of characteristic differences in land cover, elevation, and temperature between HLU, AR/P values were selected for each HLU independently. For the WML, 0.15 AR/P was found to be the most reasonable ($R_{WML} = 85$ mm/yr) and 0.10 AR/P was selected for EML and SVL ($R_{EML} = 39$ mm/yr, $R_{SVL} = 32$ mm/yr). No AR was defined for the NVL ($R_{NVL} = 0$ mm/yr), due to substantially lower precipitation rates (Figure 2b) and the high ET rates expected in this high-altitude semiarid valley. Potential ET in the NVL was previously measured to be >3 times P_{NVL} [Spahr, 1981]. Huntley [1979] and Emery *et al.* [1971] estimated actual ET in the nearby San Luis Valley (50 km to the south) to be about twice that of P_{NVL} where the water table intersected the land surface. However, these studies also estimated an exponential decay in actual ET rates with depth, with negligible ET occurring below a depth of 4 m. South Park's NVL is assumed to have a similar ET decay trend and only shallow groundwater near seepage faces and surface water bodies are likely to be susceptible to significant ET during the warmer summer months. As such, ET was not directly simulated over the surface of the NVL, but the seepage and surface water boundary condition described in the following sections allow water to leave the basin, where ET is assumed to consume a large portion of this discharge. It remains possible that some AR may occur below snowdrifts in early spring when ET is unlikely to occur. These drifts are expected to be small relative to the regional scale of the model, and the simulation of sub-landscape recharge patterns is beyond the scope of this study.

3.1.3. Seepage Boundary Conditions

Groundwater discharge as seepage was permitted across the entire model surface as a constrained constant-head boundary condition, where hydraulic head is defined by the reference elevation of the land surface when the direction of the fluid flux normal to the upper layer is outward. If the fluid flux direction is inward, the boundary condition remains inactive and head is undefined. Conceptually, this model seepage encompasses flow to springs and seeps, interflow, vadose zone processes, and ET.

3.1.4. Surface Water Boundary Conditions

Streams and reservoirs act as both focused sources and sinks of groundwater within the South Park basin, and shallow groundwater and surface water were assumed to be in close communication. Stream gage records indicate mountain streams are perennial to at least 3150 m elevation (NWIS data, three sites) and runoff from snowmelt makes substantial contributions to stream flow throughout the warmer months and may provide focused recharge to valley aquifers. Similar timing of events between available groundwater and stream hydrographs (NWIS data) [Bruce and Kimbrough, 1999; Chapman *et al.*, 2003] and stable isotope and major ion chemistry of water sampled in NVL fens [Chapman *et al.*, 2003] support the assumption of surface-groundwater communication in the valley. As such, model elements along streams and large lakes ($>30,000$ m²) were assigned constant-head boundary conditions coincident with the land-surface elevation. Tributaries that do not extend into the WML do not have access to reliable snowmelt runoff and may be ephemeral. A flux-direction constraint was added to these boundary conditions identical to the seepage boundary condition, preventing ephemeral streams from acting as focused recharge sources while still permitting groundwater discharge to the stream if the hydraulic head of the surrounding aquifer favors it.

3.2. Hydrostratigraphy

Complex stratigraphy and geologic structures present particular challenges to understand the role geology plays in groundwater flow through folded and faulted bedrock aquifers. The geologic complexity of South Park's valley is the result of a sequence of depositional and erosional periods punctuated by multiple orogenic and volcanic events. A wide variety of sedimentary rock types and extensive folding and faulting translate into a distinctive and heterogeneous permeability field. Permeability is one of the most significant hydraulic parameters in mountain groundwater flow models [Forster and Smith, 1988a] and also one of the most difficult to define. A 3-D geologic model of the basin was developed to populate the permeability structure of the groundwater model domain. A basin-wide bedrock map was compiled (Figure 2c) and five cross sections of major geologic units and structures were drawn, constrained by available borehole stratigraphic logs, mapped geology, and regional potential field geophysical data. Detailed discussion of the cross section development and geologic model creation is provided in Ball [2012, Appendix 4A].

Table 1. Hydraulic Conductivity (K) Values Assigned to Each Hydrostratigraphic Unit (HU) for Layer 1

HU	K (m/s)	HU Description
1	5.80E-07	Proterozoic crystalline rock aquifers
2	8.00E-08	Paleozoic aquitards
3	2.30E-06	Pennsylvanian-Permian aquifers
4	6.00E-08	Jurassic and Cretaceous aquitards
5	2.30E-06	Upper Cretaceous and Tertiary aquifers
6	2.30E-06	Tertiary volcanic aquifers
7	2.30E-06	Tertiary lacustrine aquifer

Conceptualization of geology and related permeability structure requires consideration of the scale of interest. Geologic units were grouped into major hydrostratigraphic units (HU) to facilitate regional-scale modeling (Figure 3). Because of the scarcity of aquifer hydraulic test data, the creation of HUs was completed using two qualitative criteria: (1) rock types likely to have similar hydraulic properties that occur in stratigraphic succession were generally grouped into the same HU; and (2) the estimated maximum thickness of

each geologic unit was considered, and those less than 500 m thick were combined with surrounding geologic units. The HU designations were applied to the geologic model to create a 3-D hydrostratigraphic model (Figure 4). Bedrock HUs were assumed to extend to the land surface. Thin, mostly unsaturated unconsolidated glacial and alluvial deposits that occur in parts of the valley were not directly simulated. We acknowledge that these unconsolidated materials are likely to be relatively high in permeability and may conduct groundwater locally where they lie below the water table; however, the typical saturated thickness of these deposits (<15 m) did not warrant creation of a unique HU at this scale.

This conceptualization captures the regional geologic framework and structural style of the basin while minimizing local-scale complexity in the permeability field. Local-scale geologic structures, such as hydrologically distinct fault zones and small folds, may be hydrologically significant in the immediate vicinity of that structure, particularly under hydraulic stress. Similarly, hydraulic properties are likely to vary within a given geologic formation, but this variability cannot be spatially constrained without detailed measurements and are likely not critical to capture regional flow processes.

Hydraulic conductivity (K) values were uniformly assigned to each HU to represent the regional permeability structure. The final values were chosen through trial-and-error model calibration with a strong consideration for previously published values of similar rock types (Table 1). The regional-scale estimates presented by Gleeson *et al.* [2011] were considered to be particularly applicable to the scale of the South Park basin model. Each HU was initially matched to Gleeson *et al.*'s hydrogeologic categories and corresponding mean K values. These values were found to be reasonable when compared to the limited number of K estimates from local hydraulic tests in the fractured crystalline rock (HU1) and South Park Formation (HU5) [Ball *et al.*, 2010; Jehn, 1997; Marler and Ge, 2003] and various estimations from similar rock types in nearby basins [Bossong *et al.*, 2003; Huntley, 1979].

The mean K values reasonably simulated observed water table elevations for a variety of boundary condition assignments, although some adjustments had to be made to avoid unreasonable water table configurations and model convergence errors. The K of the first two layers (upper 200 m) of HU1 was raised by 1 order of magnitude in comparison to the reported mean K of crystalline rock in an effort to represent a near-surface zone of increased fracture intensity. The K of the two primary aquitards units (HU2 and HU4) were raised by 0.5 and 2 orders of magnitude from the mean reported values, respectively, to improve numerical stability.

Reduction in K with depth is supported locally by data from Robinson [1978] and from fluid and heat flow modeling studies [Davis and Turk, 1964; Ingebritsen and Manning, 1999; Saar and Manga, 2004]. This reduction may have substantial impacts on the dynamics between local, intermediate, and regional flow systems within the basin [Jiang *et al.*, 2009]. The relation developed by Ingebritsen and Manning [1999] and later validated by Saar and Manga [2004] for depths >1 km was used to define the power law reduction in K with depth below 1 km. For model layers above 1 km, a constant K was applied for numerical stability and simplicity, with the previously described exception of simulated highly fractured rock in the upper two layers of HU1.

3.3. Assessment of Model Performance

Observed hydrologic conditions from well and stream data were used to refine the assigned parameters in the reference model and to estimate the model's performance at capturing the known characteristics of the basin-scale groundwater flow system. Several parameters were adjusted within physically reasonable bounds, including (1) K contrasts between HUs, (2) AR/P values for each HLU, (3) stream boundary

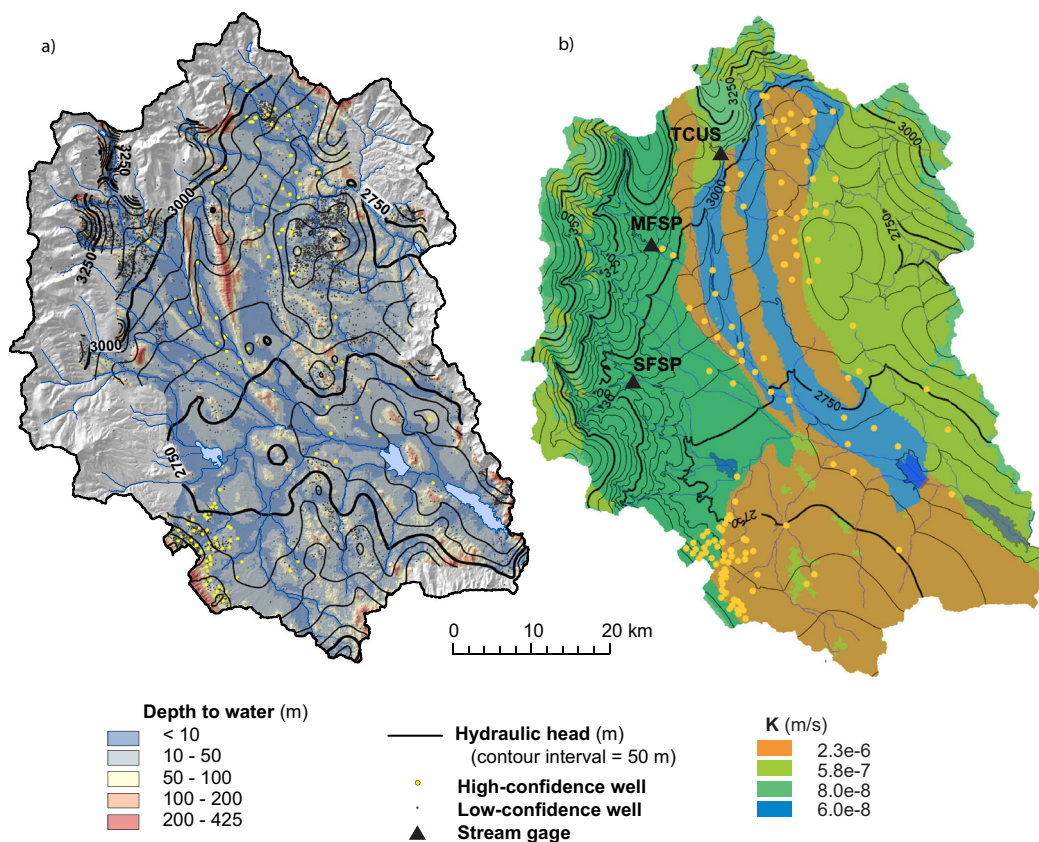


Figure 5. Maps of the South Park basin showing water table elevation contours from (a) observed well and stream data and (b) the reference numerical groundwater flow model. Depth-to-water and K of model layer 1 are also shown in Figures 5a and 5b, respectively. Streams (thin blue lines) and lakes (blue polygons) are shown with the locations of high-confidence wells and stream gages used to determine goodness of fit. Contouring was not attempted in Figure 5a for mountainous regions due to a lack of wells. (South Fork of the South Platte River, SFSP; Middle Fork of the South Platte River, MFSP; and Tarryall Creek at Upper Station, TCUS.)

conditions, and (4) the addition of explicitly simulated ET. Where notable improvements to model performance were not achieved, the simplest model with the smallest range of parameter values was chosen. Through numerous manual adjustments and runs, an understanding of the model response was developed until the most appropriate set of parameters was obtained in fitting the observed data.

A contour map of observed water levels in wells was created to establish the known water table configuration within the bedrock aquifers of the basin. Depth-to-water measurements from 5288 wells were compiled from three data sources and were assumed to represent steady state, unconfined water table conditions: (1) personally collected water level data (16 wells), (2) water level data reported by the NWIS (136 wells, NWIS data), and (3) static-water levels reported in well-permit registration forms on record with the Colorado Division of Water Resources (5136 wells, <http://www.dwr.state.co.us/WellPermitSearch/>). The first two data sources were originally collected for scientific purposes, have undergone previous quality control measures to avoid hydraulic stress conditions, and are considered to be high confidence measurements. Water levels reported from well permits are less reliable and include estimates made during drilling or well development and may reflect 10 to 100s of meters of divergence from steady state conditions. These data are considered lower confidence and underwent statistical culling to remove localized outliers before being included in contouring. DEM elevations were enforced on the contours to prevent the water table contours from exceeding the land surface. Essentially no well data were available for the mountainous regions of the model domain, and the water table in these regions is undefined in Figure 5a.

The compiled water level data and water table contours were used to quantify the statistical performance of the reference model at well locations and to qualitatively assess the model's ability to capture the observed regional water table configuration. The model achieved reasonable goodness of fit when

compared to high-confidence measurements: normalized root mean square error (NRMSE) = 6.0%, coefficient of determination (r^2) = 0.90. Qualitatively, the model reasonably captures the regional patterns identified in the observed water table contour map (Figure 5). The model generally succeeds at simulating the observed character of groundwater-stream interactions and the relative hydraulic gradients across the various HUs. These similarities support the conceptualized K structure near the model's surface, the relative recharge distribution, and assigned stream boundary conditions.

Maintaining reasonable goodness of fit at well locations was possible using a wide range of model parameters. Because these data points are mostly located in the valley or near streams, stream boundary conditions were the most important parameter in achieving good model performance using these criteria. The explicit simulation of ET to the NVL was the other main parameter to which hydraulic head near wells was sensitive, resulting in less favorable goodness of fit. Changes in K contrasts, recharge rates, and other boundary conditions had limited impact on goodness-of-fit statistics at low-elevation wells.

Model performance in the WML remained difficult to evaluate using observed well data. The water table position relative to the land surface varies greatly in the numerical model, from about 500 m to over 800 m depth below mountain summits and about 100 m to nearly 300 m below passes, while intersections between the water table and land surface commonly occur in the incised mountain valleys. While no water table observations are available in the WML, observed water table depths between 90 and 130 m at nearby Webster Pass [Caine *et al.*, 2006], located about 5 km northeast of South Park at an elevation of 3687 m on the Continental Divide, suggests that the simulated water table depth below mountain passes may be reasonable for the region.

Modeled groundwater discharge as stream base flow was another primary parameter used to evaluate model performance. Although there are far fewer unregulated stream gages than wells, gage data do exist for the mountain landscapes. Mean daily base flow was estimated from the seasonal lows reported in perennial stream discharge records (USGS NWIS data) at three gages in the WML (Figure 5). Base flow estimates were compared to modeled groundwater discharge to stream valleys upstream of the gage location. The balance of fluid fluxes leaving and entering model nodes within 50 m of the stream was used to estimate the groundwater discharge contribution to selected mountain stream reaches with full-year gage records. The 50 m threshold was selected by qualitatively assessing typical widths of valley bottoms below known perennial conditions and the extent of marshy areas above tree line. Discharge that occurs more than 50 m upslope of streams is considered seepage in the analysis. We acknowledge that a large portion of the seepage component likely migrates toward streams as overland flow or interflow after being exposed to surface and vadose zone processes.

The high elevation gage data from the Middle and South Forks of the South Platte River (MFSP, SFSP) are reasonably well simulated by the reference model, with modeled base flow within 11 and 9% of the observed values, respectively. Both of these watersheds share similar proportions of HU1 (crystalline aquifer) and HU2 (Paleozoic sedimentary aquitards), and the modeled base flow supports the ratio between assigned recharge rates and K. The extent of discharge zones further suggests that the Middle and South Forks are perennial to elevations of 3450–3550 and 3300–3400 m, respectively. The other high elevation gage, Tarryall Creek at Upper Station (TCUS), is not well simulated in the calibrated model and is under predicted by nearly 50%. As base flow at the other gages and valley water table configurations were reasonably simulated, additional alterations in model K and boundary conditions were not made to improve model performance with respect to this watershed.

3.4. Alternative Model Development

Studies of intermountain and mountainous basins like South Park are often hindered by the sparse distribution of well data in high elevation areas. Although the water table configuration and goodness-of-fit statistics suggest that the reference model reasonably simulates groundwater flow in the South Park basin, the water table position in the mountainous parts of the basin remains unobserved, and the model is therefore poorly constrained in the mountain landscapes. Five alternative numerical flow models were developed to simulate regional groundwater flow under different mountain water table elevations, specifically in the WML. The objectives of the alternative models are (1) to test the relative importance of quantifying poorly observed mountain water tables in the regional-scale hydrology of intermountain basins and (2) to gain

Table 2. Basin-Wide and HLU-Specific Water Balances Normalized by Basin Total Recharge and HLU Total Recharge^a

Water Balance Component		South Park Basin	WML	NVL	SVL	EML
<i>% Basin-Wide Total Recharge</i>						
In	AR	89.7	53.4	0.0	15.6	20.6
	FR	10.3	0.0	7.8	0.1	2.1
Internal Transfer	MBR (in)	0.0	0.0	11.4	0.6	2.9
	MBR (out)	1.5	9.3	1.5	3.9	2.3
Out	GW	1.5	-	-	-	1.5
	BF	38.9	13.8	7.0	5.9	12.3
	Seepage	59.6	30.5	11.1	6.7	10.0
<i>% HLU Total Recharge</i>						
In	AR	-	99.3	0.0	96.1	80.4
	FR	-	0.7	40.5	0.3	8.1
Internal Transfer	MBR (in)	-	0.0	59.5	3.5	11.5
	MBR (out)	-	17.3	7.7	23.4	8.8
Out	GW	-	-	-	-	5.7
	BF	-	25.7	35.5	35.6	47.1
	Seepage	-	57.0	56.8	40.9	38.4

^aAreal recharge, AR; focused recharge from streams, FR; mountain block recharge, MBR; groundwater flow to eastern domain boundary, GW; stream base flow, BF; western mountain landscape, WML; northern valley landscape, NVL; southern volcanic landscape, SVL; and eastern mountain landscape, EML.

insight into the sensitivity of valley aquifers in a fold and fault belt to different hydrologic conditions in the mountain block, the primary source of recharge to valley aquifers.

Previous studies have shown that water table elevations vary as a function of recharge to permeability [Haitjema and Mitchell-Brucker, 2005; Gleeson and Manning, 2008], and as such, simulating the impact of mountain water tables on regional groundwater flow through both mountain and valley aquifers can be accomplished by changing AR rates alone. Because the WML is modeled with a relatively uniform permeability structure, particularly in comparison to the heterogeneous valley and volcanic landscapes, changing K values in the WML would likely result in similar regional trends as those developed using the alternative mountain AR scenarios. Furthermore, climate change has the potential to impact the AR rates through changes in total precipitation, soil moisture, snowmelt timing, and shifts in precipitation states between snow and rain. These alternative models allow us to examine how changing mountain AR rates may impact mountain, valley, and basin-wide groundwater flow.

Alternative model scenarios were developed using the reference model as a starting condition and systematically varying the AR rate assigned to the WML. Five scenarios were developed ranging from relatively dry (0.05 and 0.1 AR/P) to relatively wet (0.2, 0.3, and 0.4 AR/P) mountain conditions in comparison to the reference model (0.15 AR/P). These AR/P ranges were bounded by previously published estimates of AR efficiency in semiarid basins compiled by Scanlon et al. [2006] and Wilson and Guan [2004]. Goodness-of-fit statistics, stream base flow, water table elevations, and water balance configurations were evaluated for all models using identical procedures and sample sets used in the evaluation of the calibrated model.

4. Results

The reference groundwater flow model was used to calculate water balances for the entire model area and for each individual HLU (Table 2 and Figure 6). The water balances quantify inflows (AR and focused recharge from streams), outflows (seepage, stream base flow, groundwater underflow from the eastern domain boundary), and internal groundwater transfers between landscapes (MBR). Each water balance component has been normalized to basin total recharge to illustrate the major processes with respect to the basin (Table 2 and Figure 6a). The HLU-specific balances have also been normalized to HLU total recharge to illustrate the relative importance of each water balance component within a given landscape (Table 2 and Figure 6b).

Basin-wide, AR dominates inflow while only 10% comes from focused recharge in losing streams, predominantly delivered to aquifers in the valley (Table 2). The majority of outflow is through a combination of

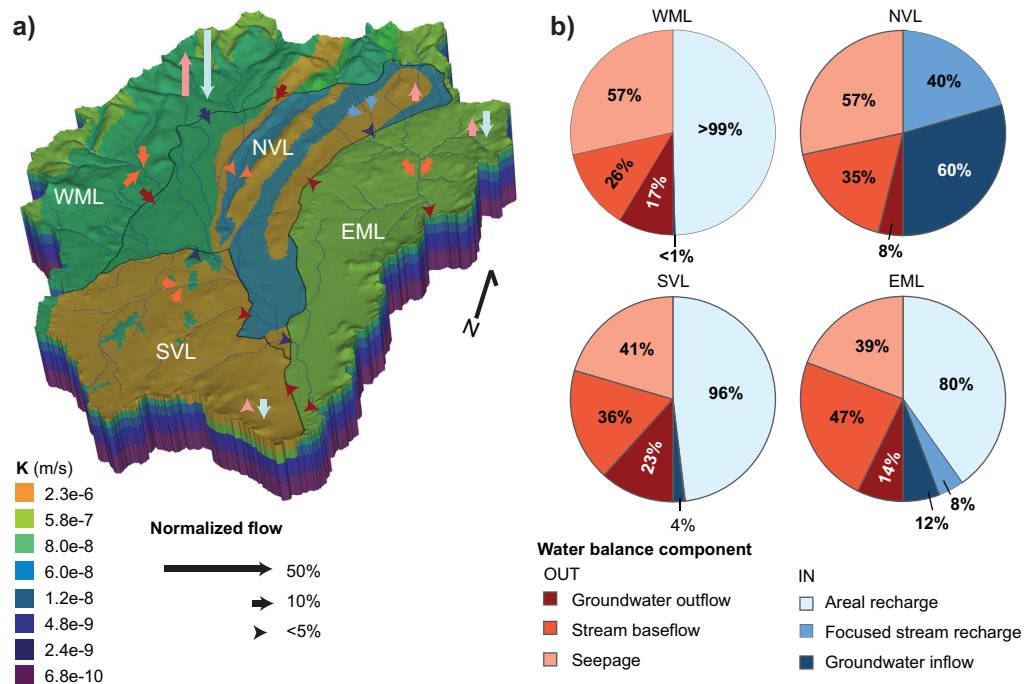


Figure 6. Conceptual distribution of groundwater recharge and discharge in the reference model showing (a) exchanges between HLU units through proportional arrows for each water balance component normalized by total model recharge and (b) HLU-specific water balances normalized by total HLU recharge. Supporting data are given in Table 2. (Western mountain landscape, WML; eastern mountain landscape, EML; northern valley landscape, NVL; and southern valley landscape, SVL.)

surface seepage (59%) and stream base flow (39%). Groundwater flow is generally directed toward the valley where it discharges to streams and observed wetland areas, and <2% of the total recharge leaves the model as groundwater underflow through the constant head boundary conditions corresponding to the reservoir outlets at the model domain’s eastern perimeter. This limited groundwater flow is shallowly focused in the stream valleys, where 55% of the flow occurs in the first 500 m and <10% occurs below 2 km.

The water balances of individual HLU highlight some of the fundamental differences between groundwater flow systems developing under different landscape conditions. Higher average precipitation and AR rates in the WML result in higher total groundwater fluxes in comparison to the other HLU (Table 2). AR accounts for essentially all recharge in the WML and for 53% of the total basin recharge across all landscapes. The majority of WML recharge circulates through local and intermediate flow systems where it discharges to streams and seepage faces in the incised mountain valleys (Figure 6 and Table 2). About 17% of groundwater recharge entering the WML travels through intermediate to regional flow systems and is transferred primarily to the NVL as mountain block recharge (MBR). Similar to the WML, AR dominates total recharge to the SVL. Seepage is less prominent in the SVL than in the WML (41% compared to 57%).

MBR is the primary recharge mechanism to valley aquifers in the NVL, estimated to be 60% of its incoming water (Figure 6b). Focused recharge through losing streams accounts for an additional 40% of the inflow in the valley, and these losing reaches are mostly focused in the Cretaceous and Tertiary aquifers of HU5. Flow predominantly leaves the NVL through seepage and stream base flow, and gaining stream reaches are particularly prominent where streams pass over the low-permeability shales of HU4. The groundwater flow direction is mostly subparallel to the boundary between the EML and NVL, and the groundwater flow into the EML is limited and occurs shallowly near rivers that pass across the landscape boundary (Figure 6).

The recharge distribution of the EML is more diverse than that of the WML and SVL. About 80% of flow in the EML is sourced through AR, while the remaining recharge enters through groundwater underflow and limited losing reaches of the high-order streams draining the majority of the basin. The incision of streams results in mostly gaining-stream conditions, where 47% of the EML’s groundwater is discharged, however,

Table 3. Alternative Mountain Areal Recharge Model Scenarios and Goodness-of-Fit Statistics With Respect to Water Table Observations in Wells^a

AR/P	AR Rate (mm/yr)	r ²	NRMSE (%)
0.05	28	0.87	6.6
0.10	56	0.89	6.0
0.15	85	0.90	6.0
0.20	112	0.90	5.9
0.30	168	0.90	5.9
0.40	224	0.90	5.9

^aAreal recharge, AR; precipitation, P; normalized root mean square error, NRMSE; and linear regression goodness of fit, r².

the EML has lower topographic relief than the WML, and seepage is less prominent (Table 3). A total of 14% of EML recharge leaves the EML through groundwater transfers: 8% transfers to the NVL as MBR across the major fault dividing the two landscapes, while 6% leaves the model where the stream valleys intersect the eastern boundary (1.5% of the basin total recharge).

The vertical distribution of MBR was examined by sampling the magnitude of fluid flux between the HLU interfaces surrounding the NVL. The

total flow volume passing horizontally across each HLU interface for a given model layer was sampled, and percentages of flow for each HLU interface were calculated to examine the relative distribution of flow with depth (Figure 7a). To make direct comparisons of flow magnitude between different HLU interfaces without introducing a bias to model layer size or the geographic extent of a given HLU interface, the volumetric flow of each interface layer was normalized by the total length of the interface and the layer thickness (Figure 7b). This leads to volumetric rates reported as m³/(d × m × m), or m/d.

Across all interfaces, the majority of flow is focused in the upper saturated 1 km (Figure 7). However, deeper and more uniform distribution was driven by higher elevation terrain. The SVL has the overall lowest land surface elevation in comparison to the EML and WML, and relative flow sharply declines to <15% below saturated depths of 500 m (Figure 7a). In contrast, the groundwater driven out of the high terrain of the WML circulates more deeply and uniformly, where 29% circulates below 1 km, and a substantial amount of flow reaches the valley through intermediate-scale MBR. However, less than 10% of the total flux passes below 2 km. The vast majority of MBR leaving the WML leads to discharge locations at internal streams and seeps in the valley, and negligible groundwater volumes are driven below the NVL as deeply circulating groundwater flow to the eastern model boundary (Figure 8).

Model performance was reevaluated for the alternative mountain AR scenarios. Mean water table elevations in the WML rose logarithmically over 255 m between the wettest and driest models, with the largest variations occurring below mountain summits (Figure 9a). Despite the large fluctuations in mountain water tables, model goodness of fit with respect to observed water table elevations in wells was effectively unchanged over the range of simulated mountain AR (Table 3) with the exception of the driest model

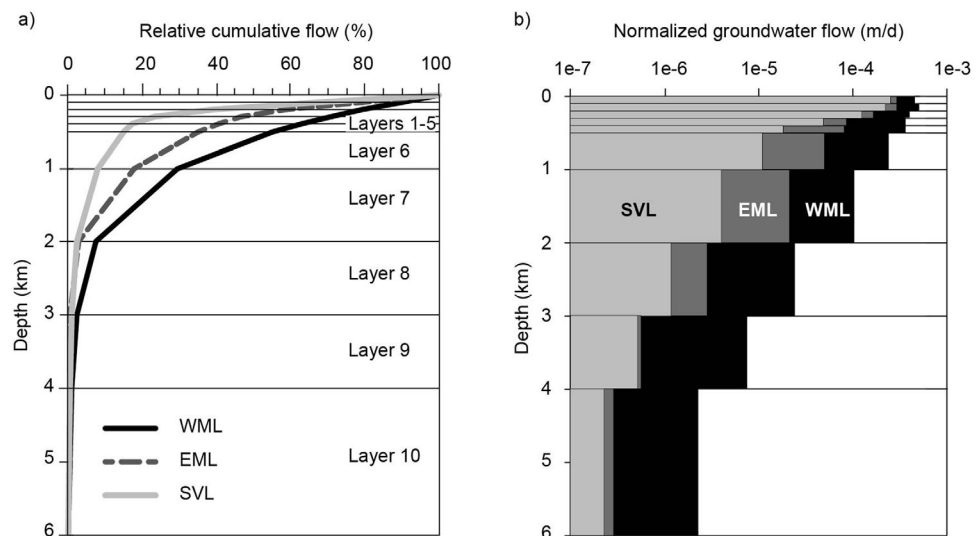


Figure 7. Graphs showing (a) the relative cumulative groundwater flow and (b) total volumetric flow normalized by interface length and layer thickness contributing to the northern valley landscape (NVL) for the interfaces between hydrologic landscapes in the reference model. (Western mountain landscape, WML; eastern mountain landscape, EML; and southern volcanic landscape, SVL.)

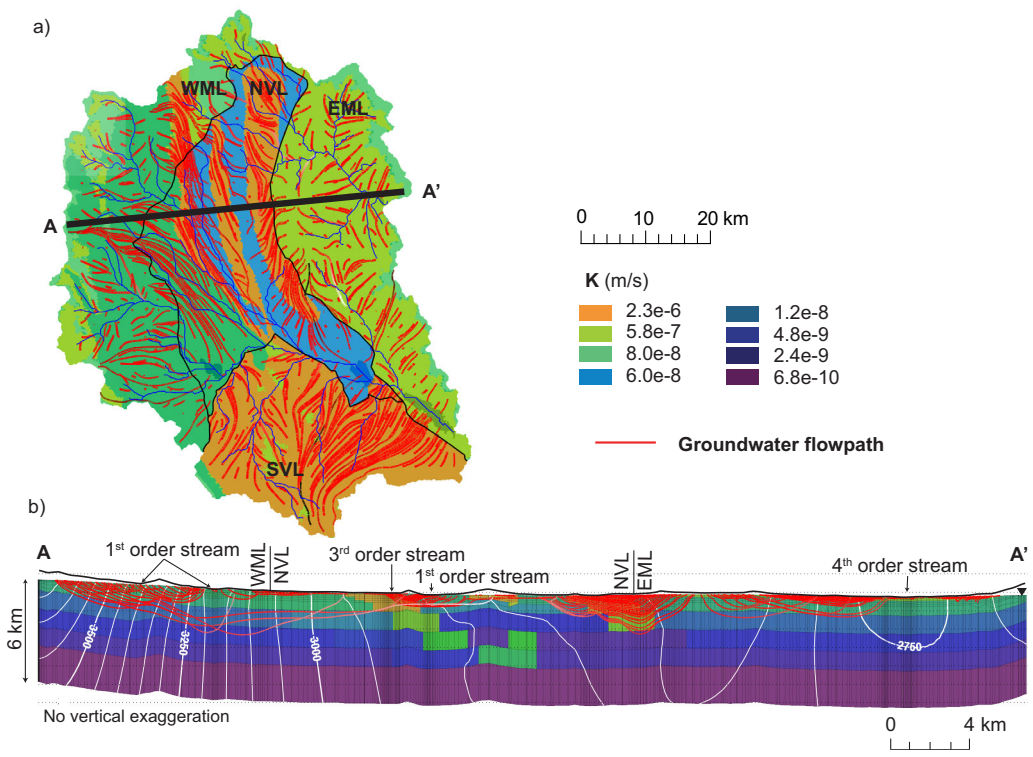


Figure 8. (a) Plan view map and (b) cross section showing groundwater flow paths and hydraulic head contours (50 m contour interval, white lines) using the reference model. In the NVL, groundwater predominantly flows down-valley through the folded and faulted aquitards and many flow paths in Figure 8b are oriented perpendicular to the cross section and not visible. (Western mountain landscape, WML; eastern mountain landscape, EML; northern valley landscape, NVL; and southern valley landscape, SVL.)

showing weaker fit statistics. Stream discharge and perennial flow elevations estimated at mountain stream gages showed more sensitivity to mountain AR rates (Figures 9b and 9c). Mean perennial stream extents increased linearly with increasing AR/P over 250 m. All three gages show large variations in simulated discharge relative to observed base flow. The gages with the largest drainage area and observed base flow, MFSP and SFSP, show reasonable discharge estimates between 0.15 and 0.20 AR/P. Wetter and drier models led to base flow estimates much more divergent from observations at these gages. Base flow at TCUS is best simulated by 0.30 AR/P. TCUS has a substantially smaller drainage area and lower observed base flow than the other gages (9870 m³/d compared with 13,150 m³/d (SFSP) and 18,950 m³/d (MFSP)). This watershed is also collocated with the highest PRISM precipitation averages in the basin (Figure 2b). The illustrated preference for higher AR rates at TCUS in comparison with the other two gages indicates that the landscape-wide averaging of AR rates may be less appropriate as smaller subareas of the model are evaluated. This watershed also contains a major fault zone in the northernmost extent of the fold and fault belt, and the permeability structure was highly simplified in the regionalization of model K. These simplifications may not be appropriate for considering discharge at the watershed scale.

5. Discussion

5.1. Landscape and Structural Controls on Groundwater Flow

Simulated groundwater flow patterns between the mountain and valley landscapes have substantially different characters. In the mountain landscapes, topographically controlled nested flow systems [e.g., *Toth*, 1963] connect recharge areas to seepage and stream discharge locations in the valleys of low-order streams over predominantly local to intermediate scales. The short groundwater flow paths shown in Figure 8a illustrate these local-scale flow systems and show their correlation to seepage faces and low-order streams (Figures 8a and 10). Some regional-scale flow paths from the highest terrain of the WML bypass the local mountain valleys to become MBR through regional flow, but much of the MBR occurs through intermediate

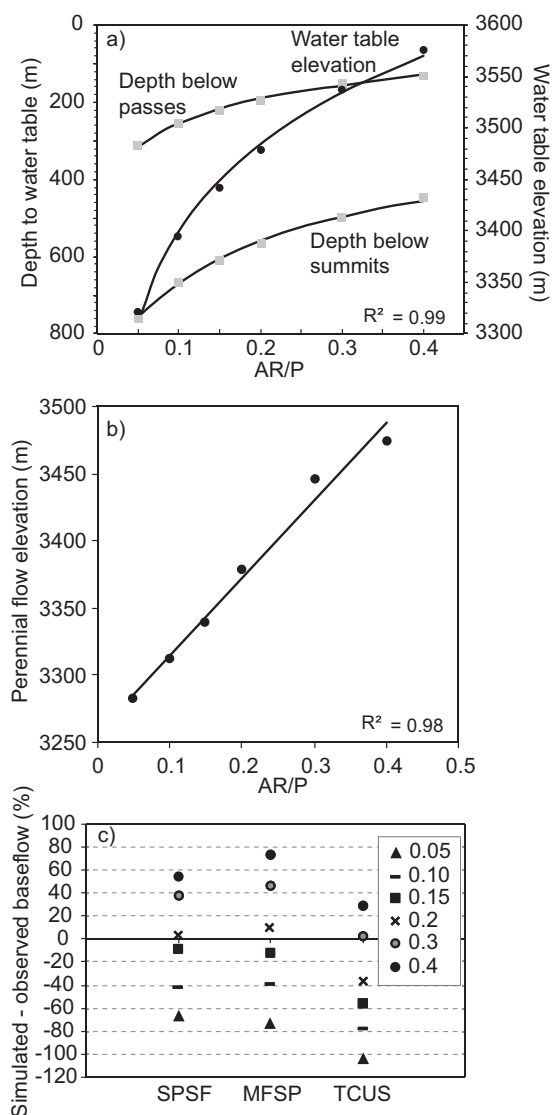


Figure 9. Comparison between alternative mountain AR scenarios showing (a) mean depth to the water table below mountain passes and summits and mean mountain water table elevations, (b) mean elevation of perennial flow on gaged mountain streams, and (c) percent difference between observed and simulated stream base flow on gaged mountain streams. (South Fork of the South Platte River, SFSP; Middle Fork of the South Platte River, MFSP; Tarryall Creek at Upper Station, TCUS; and areal recharge-to-precipitation ratio, AR/P).

flow from recharge areas closer to the mountain front. *Welch and Allen* [2012] reached similar conclusions in groundwater flow models of small subwatersheds of the Okanagan basin of British Columbia, Canada. The cross section shown in Figure 8b further illustrates that local and intermediate systems predominantly circulate groundwater in the upper 2 km below the water table, while limited regional-scale flow toward the valley circulates more deeply (Figure 7).

The permeability structure created by the valley fold and fault belt translates into a series of isolated aquifers surrounded by extensive aquitards and places substantial control on simulated groundwater flow patterns in the NVL. Figure 8a shows the alignment of flow along the axes of the fold and fault belt, while the limited topographic relief prevents the formation of clear nested flow systems. This structural control tends to cause shallow water tables and the development of seepage by limiting groundwater flow between aquifers, particularly in the aquifers in the western part of the valley (Figure 10). This structural control also influences the relative contribution of different recharge mechanisms to different aquifers. Areal recharge contributes to the northern parts of the Pennsylvanian-Permian aquifers (HU3) where they extend into the WML (Figure 2c). These aquifers also coincide with zones of substantial MBR. In contrast, the structurally isolated Cretaceous and Tertiary aquifers

(HU5) are mostly recharged through losing streams, and the low-permeability Jurassic and Cretaceous aquitards limit groundwater flow and MBR from the western mountains (Figure 8). While some MBR from the EML recharges the eastern part of these aquifers near the center of the basin where hydraulic gradients drive flow across the HLU interface, the total flow across the EML boundary is small compared to the losing stream contributions.

The SVL has some unique characteristics compared with both the mountain and valley landscapes. SVL flow paths show less pronounced local flow systems and longer groundwater flow paths than seen in the mountains (Figure 8a). However, the relatively uniform and shallow permeability structure used to simulate the volcanic deposits that mantle this region prevent the development of obvious permeability controlled flow paths. The combination of reduced topographic incision and surface roughness and higher shallow K leads to fewer intersections between the land surface and water table, reducing seepage (Figure 10). As a result, a

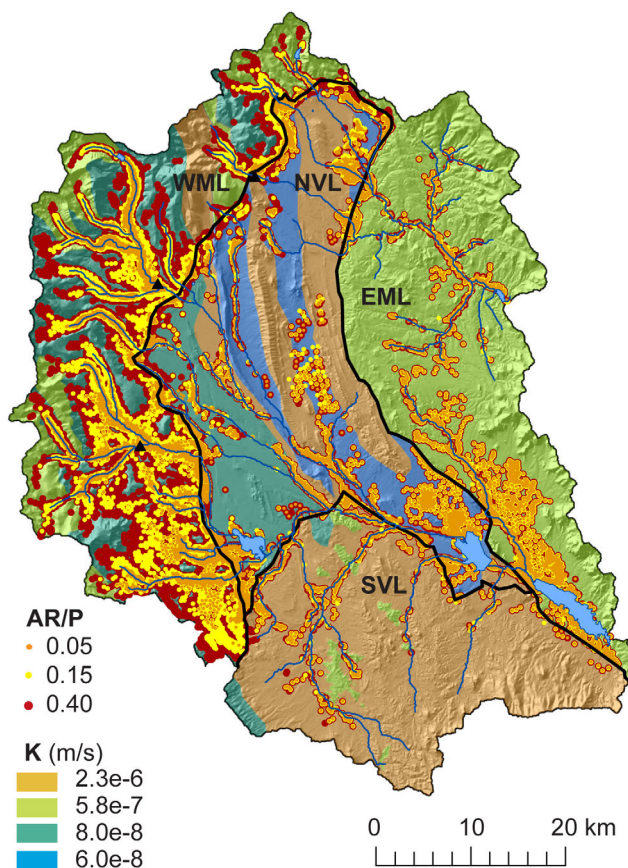


Figure 10. Seepage distribution for the 0.05, 0.15, and 0.4 AR/P mountain recharge scenario models. (Western mountain landscape, WML; eastern mountain landscape, EML; northern valley landscape, NVL; and southern valley landscape, SVL).

higher percentage of flow in the SVL is discharged to streams or is able to remain in the saturated flow system to pass to the valley (Table 2 and Figure 6b).

The South Park model illustrates that the susceptibility of fold and fault belt aquifers to hydrologic stress will in part depend on their structural position and the relative dominance of different recharge mechanisms. Change in stream flow is one example of a hydrologic stress. Climate change may affect mountain snow packs, the form of precipitation, and the timing and total stream discharges associated with spring snowmelt [i.e., Hay et al., 2011; Pederson et al., 2013]. Structurally isolated aquifers are likely to be more strongly impacted by such changes in stream discharge because of their structural position. The aquitards of the fold and fault belt limit groundwater flow into these aquifers from adjacent areas, causing

focused recharge from losing streams to become the dominant recharge mechanism. Because of the dynamic nature of stream flow and the short travel times required for stream discharge to reach the valley from snowmelt and runoff in the mountains, the groundwater systems of these structurally isolated aquifers are also likely to be more susceptible to short-term climatic variability than aquifers with other recharge sources in other structural positions. The aquifers on the outer perimeter of the fold and fault belt and those that extend into the mountain block, in contrast, receive significant MBR contributions with longer travel times. Manning [2011] has suggested that the longer travel times associated with MBR will buffer aquifers from short-term variability in stream flow or other surface conditions. As such, the groundwater flow systems of external aquifers in basins underlain by folded and faulted rocks are likely to be more resilient to short-term climatic variability than structurally isolated aquifers.

5.2. Seepage, MBR, and Mountain/Valley Interaction

Simulated seepage was observed to be the dominant discharge mechanism for the WML and NVL under all mountain AR scenarios (Figures 10 and 11). The mechanisms for producing these seepage-dominated systems are controlled by the topographic incision of the mountain valleys. Even under low AR/P (<0.15), the relatively smooth surface of the water table frequently intersected the relatively rough and incised mountain topography in the WML, leading to local flow systems and large portions of seepage relative to base flow and MBR (Figures 10 and 11). Water table elevations in western NVL remain close to the land surface elevation of stream outlets, and the low-permeability layers of the fold and fault belt limit the ability of the structurally external aquifers to drain. Seepage at the land surface near the mountain front becomes a common discharge location.

Valley incision and topographic roughness act as hydraulic controls on the interaction between model landscapes, particularly with respect to MBR to the valley. While higher mountain AR rates and resulting water

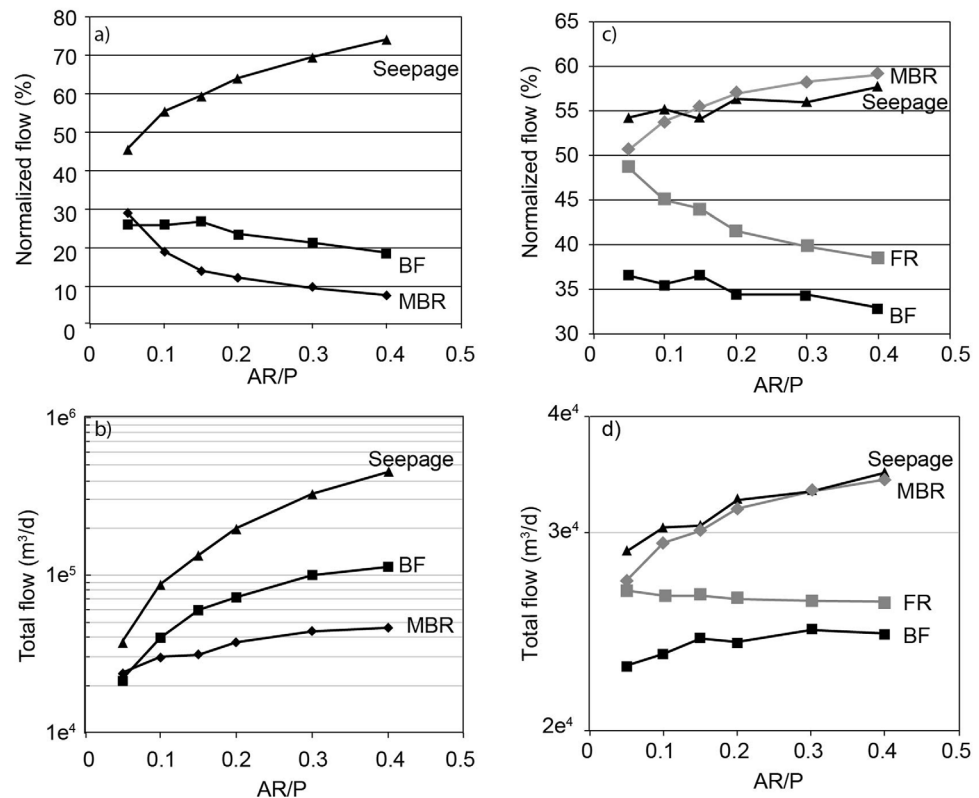


Figure 11. Trends between the alternative mountain AR model scenarios showing WML discharge water balance components (a) normalized to total WML recharge and (b) unnormalized total flow; NVL discharge (black lines) and recharge (gray lines) water balance components (c) normalized to total NVL recharge and (d) unnormalized total flow. Groundwater flow leaving the NVL experienced negligible change under all scenarios and is not shown. (Stream base flow, BF; mountain block recharge, MBR; focused stream recharge, FR, areal recharge-to-precipitation ratio, AR/P; western mountain landscape, WML; and northern valley landscape, NVL.)

table elevations drive larger total flows in all WML discharge components (Figure 11b), the relative proportions of MBR and stream base flow to WML total recharge decline as seepage becomes the dominant discharge mechanism (Figure 11a). As mountain AR rates increase, a larger portion of total recharge is directed to increasingly small, local flow systems and seepage faces, and a lower percentage of the total flow passes to intermediate and regional flow (Figure 10). The localization of mountain flow paths under increasing mountain AR rates supports the findings of Gleeson and Manning [2008] and Welch and Allen [2012] that indicate MBR increases nonlinearly with mountain AR rates. These studies used schematic models with linear landforms and uniform permeability fields in small mountain watersheds. The South Park basin model suggests that these results are valid at the scale of regional groundwater basins and under more realistic heterogeneity, including realistic topography and complex permeability structure.

The large areal and depth scales of the South Park model allow us to track the fate of increased total MBR through the mountain/valley interface, whereas the previously mentioned studies treat the valley as a boundary condition. Total flow in the NVL increased in nearly direct proportion with increasing MBR; however, this increased flow circulated primarily through the structurally external western aquifers of the fold and fault belt to discharge as seepage (Figures 10 and 11b). The flow-limiting aquitards in the fold and fault belt caused internal aquifers to remain somewhat isolated from variations in MBR. Figure 11b shows total focused recharge from streams, the primary mechanism recharging structurally internal aquifers in the NVL, to remain relatively constant under all mountain AR scenarios, indicating little change in the recharge dynamics or total flow volumes of these aquifers.

5.3. Challenges in Calibrating Mountain Groundwater Models

Groundwater flow models are nonunique. As such, a variety of model parameter settings can result in similar hydraulic head distributions. The impact of alternative mountain AR rates to basin-scale and valley flow systems highlights some important points about model sensitivity and the constraints on mountain-valley

groundwater system interactions. The consistency of goodness-of-fit statistics to well observations under the alternative mountain AR scenarios highlights this nonuniqueness and the insensitivity of water table elevations at well locations. Wells in the South Park basin, as in most intermountain basins, are limited to lower elevation areas and along stream valleys. Water table elevations in wells near streams are insensitive to most model parameters exclusive of nearby stream boundary conditions. Wells away from streams are limited primarily to the valley, where the water table is relatively shallow and primarily controlled by the land surface itself.

The driest mountain AR scenario led to a slight reduction in goodness of fit to well observations as a result of dropping water table elevations, whereas all other scenarios showed essentially equivalent goodness of fit (Table 3). Although additional analysis of the changes in water balances has shown that higher mountain AR rates do impact the main valley through increased total MBR, the closely located land-surface boundary conditions cause increasing MBR to result in increasing seepage rates (Figures 11c and 11d) and relatively fixed valley water table elevations despite fluctuations in mountain water tables exceeding 200 m (Figure 9a). This illustrates the inadequacy of typical well distributions in mountainous areas as the primary calibration criteria of intermountain basin groundwater models. Water table observations at higher elevations in the mountain block would significantly improve the calibration capabilities of mountain groundwater models. Similar conclusions have been reached in previous studies of smaller mountain watersheds [Tiedeman *et al.*, 1998; Johnson, 2007].

Base flow in mountain streams and the elevation of perennial flow was found to be more sensitive to changing recharge rates than valley water tables (Figure 9). These results suggest that improved observations of stream base flow conditions in the mountains and near the mountain front would be worthwhile criteria for improving the performance of numerical groundwater models in mountainous terrain, and economically more realistic than the installation of wells at high elevations. Larger numbers of gages over a range of elevations and long-term records covering winter periods would improve the predictive capabilities of intermountain basin models, particularly with respect to simulating mountain conditions where the largest groundwater fluxes have been shown to occur in intermountain basins.

Improved conceptualization of the groundwater contributions to mountain streams would also greatly benefit model calibration. In this study, we have limited the stream base flow component to the portion of model discharge in the bottom of valley incision, with only 50 m of contributing hillside flow categorized as stream base flow. However, surface discharge typically extends 100 s of meters above this zone (Figure 10), which we have chosen to highlight within the model seepage component. Determining the fate of this seepage is beyond the scope of this model, however, much of this seepage likely reaches the stream after interacting with surface and vadose zone processes. Isotopic studies [i.e., Uchida *et al.*, 2003] support significant interflow contributions to streams, where chemistry and timing differ from that of both groundwater discharge and overland flow. As such, the winter base flow discharge from field data used to define observed base flow in this model may underestimate true steady state groundwater discharge to streams. Similarly, modeled groundwater discharges to the valley bottom used to define simulated base flow may also underestimate true groundwater contributions to streams. Field observations of the travel distances, timing, and efficiency of the interflow component would improve the model conceptualization between seepage and stream base flow and may provide a powerful calibration data set, where valley bottom flow and seepage face length could be used together to constrain mountain AR rates and permeability estimates.

6. Conclusions

To investigate the role of realistic regional-scale hydrogeologic heterogeneity on groundwater flow in an intermountain basin underlain by sedimentary rocks deformed by contractional processes, a series of 3-D numerical groundwater flow models were developed for the 3360 km² South Park basin in central Colorado. The South Park basin was conceptualized into four major hydrogeologic landscapes: the western and eastern mountain landscapes, northern valley landscape, and southern volcanic landscape. These landscapes were selected for similarities in climate, topography, and permeability structure. Six models were presented that systematically alter areal recharge rates in the western mountain landscape over reasonable ranges for semiarid mountain flow systems relative to mean annual precipitation (0.05–0.4 AR/P). The models

otherwise share identical permeability structure, topography, and boundary conditions. These models were used to describe the relative importance of different recharge processes (AR, MBR, and focused stream recharge) and discharge mechanisms (seepage, stream base flow, and groundwater transfers to other landscapes or basins), to estimate typical groundwater circulation depths, and to explore the hydrogeologic relationship between the mountain landscapes and the valley aquifers. The models are not intended to represent the South Park basin in a predictive manner, but they highlight the basic processes and sensitivities that control groundwater flow and are likely representative of other semiarid intermountain basins underlain by deformed sedimentary rocks:

1. The simulated hydrogeologic landscapes have notably different styles of groundwater flow. The mountain landscapes are dominated by topographically controlled, nested flow systems while permeability heterogeneity in the fold and fault belt and decreased topographic roughness create permeability-controlled flow systems in the valley.
2. Dominant recharge mechanisms in valley aquifers were strongly influenced by the structural position of aquifers within the fold and fault belt, a likely characteristic feature of intermountain basins underlain by sedimentary rocks deformed by contractional processes. Focused recharge from losing streams was the dominant mechanism recharging structurally isolated valley aquifers. Aquifers in the westernmost extent of the fold and fault belt with direct hydrologic connection to the western mountain landscape were recharged primarily through MBR. Because of the differing recharge mechanisms, structurally isolated aquifers are likely to be more vulnerable to short-term hydrologic stresses, whereas aquifers closest to the mountain block are likely somewhat insulated from short-term variability through substantial contributions of MBR.
3. Groundwater discharge in the mountain landscape primarily occurs in seepage faces more than 50 m above the bottom of mountain valleys. Because of the dominance of seepage, the majority of groundwater circulation, particularly in the mountain landscapes, occurs in local-scale flow systems. These local flow systems have short travel paths and residence times and limited circulation depths.
4. Changes in mountain AR rates most strongly impact the mountain landscape. The topographic control imparted by the steeply incised mountain topography results in increasingly dominant local flow systems under higher water table conditions, causing higher AR rates to result primarily in higher mountain seepage and nonlinear increases in stream base flow and MBR to structurally external valley aquifers.
5. When mountain water tables rise under increasing mountain AR rates, limited increases in MBR to the valley lead primarily to increased seepage near the mountain-valley landscape interface. Because of flow-limiting nature of aquitards in the fold and fault belt, the effects of mountain hydrologic conditions have limited impacts on the structurally internal aquifers.
6. Typical well distributions in the valley and near streams, where domestic and agricultural wells are most commonly drilled, are inadequate for evaluating intermountain basin groundwater model performance through water table observations. The incision of mountain streams and the relatively flat valley result in land-surface and boundary condition control at most of these locations, and valley water tables were shown to be relatively insensitive to a wide range of mountain AR rates and total groundwater flow. Base flow in mountain streams, the elevation of perennial flow, and the distribution of seepage faces were found to be more sensitive to change recharge rates than valley water tables.

Acknowledgments

This work was funded under National Science Foundation grant EAR610027 to S. Ge and J. S. Caine. Discussion and review from A. Manning were very beneficial to this work, and thanks are extended to one anonymous reviewer for their constructive comments. Any use of trade, product, or firm names is for descriptive purposes only and does not imply endorsement by the U.S. Government.

References

- Ball, L. B. (2012), Groundwater flow in an intermountain basin: Hydrological, geophysical, and geological exploration of South Park, PhD dissertation, 255 pp., Dep. of Geol. Sci., Univ. of Colorado, Boulder, Colo.
- Ball, L. B., S. Ge, J. S. Caine, A. Revil, and A. Jardani (2010), Constraining fault-zone hydrogeology through integrated hydrological and geoelectrical analysis, *Hydrogeol. J.*, 18(5), 1057–1067.
- Belitz, K., and J. D. Bredehoeft (1988), Hydrodynamics of Denver basin: Explanation of subnormal fluid pressures, *AAPG Bull.*, 72(11), 1334–1359.
- Bosson, C. R., J. S. Caine, D. I. Stannard, J. L. Flynn, M. R. Stevens, and J. S. Heiny-Dash (2003), Hydrologic conditions and assessment of water resources in the Turkey Creek Watershed, Jefferson County, Colorado, 1998–2001, *U.S. Geol. Surv. Water Resour. Invest. Rep.*, 03-4034, 148 pp.
- Bruce, B. W., and R. A. Kimbrough (1999), Hydrologic and water-quality data for surface water, ground water, and springs in north-central Park County, Colorado, April 1997–November 1998, *U.S. Geol. Surv. Open File Rep.*, 99-183, 37 pp.

- Bryant, B., L. McGrew, and R. A. Wobus (1981), Geologic map of the Denver 1 × 2 quadrangle, north-central Colorado, *U.S. Geol. Surv. Misc. Invest. Ser.*, I-1163.
- Caine, J. S., A. H. Manning, P. L. Verplanck, D. J. Bove, K. G. Kahn, and S. Ge (2006), Well construction information, lithologic logs, water level data, and overview of research in Handcart Gulch, Colorado, An alpine watershed affected by metalliferous hydrothermal alteration, *U.S. Geol. Surv. Open File Rep.*, 2006-1189, 14 pp.
- Carceller-Layel, T., C. Costa-Alandí, P. Coloma-López, M. A. García-Vera, and J. San Román-Saldaña (2007), Groundwater in the central sector of the Ebro Basin, *Int. J. Water Resour. Dev.*, 23(1), 165–187.
- Chapman, J. B., B. Lewis, and G. Litus (2003), Chemical and isotopic evaluation of water sources to the fens of South Park, Colorado, *Environ. Geol.*, 43(5), 533–545.
- Cooper, D. J. (1996), Water and soil chemistry, floristics, and phytosociology of the extreme rich High Creek fen, in South Park, Colorado, U.S.A., *Can. J. Bot.*, 74(11), 1801–1811.
- Daly, C., W. P. Gibson, G. H. Taylor, G. L. Johnson, and P. Pasteris (2002), A knowledge-based approach to the statistical mapping of climate, *Clim. Res.*, 22(2), 99–113.
- Davis, S. N., and L. J. Turk (1964), Optimum depth of wells in crystalline rocks, *Ground Water*, 2, 6–11.
- Diersch, H. J. G. (1998), *FEFLOW Reference Manual*, 292 pp., DHI-WASY GmbH, Berlin.
- Emery, P. A., A. J. Boettcher, R. J. Snipes, and H. J. J. McIntyre (1971), Hydrology of the San Luis valley, south-central Colorado, *U.S. Geol. Surv. Hydrol. Invest. Atlas*, HA-381, 2 pp.
- Forster, C., and L. Smith (1988a), Groundwater-flow systems in mountainous terrain: 2. Controlling factors, *Water Resour. Res.*, 24(7), 1011–1023.
- Forster, C., and L. Smith (1988b), Groundwater-flow systems in mountainous terrain: 1. Numerical modeling technique, *Water Resour. Res.*, 24(7), 999–1010.
- Gillespie, J., S. T. Nelson, A. L. Mayo, and D. G. Tingey (2012), Why conceptual groundwater flow models matter: A trans-boundary example from the arid Great Basin, western USA, *Hydrogeol. J.*, 20(6), 1133–1147.
- Gleeson, T., and A. H. Manning (2008), Regional groundwater flow in mountainous terrain: Three-dimensional simulations of topographic and hydrogeologic controls, *Water Resour. Res.*, 44, W10403, doi:10.1029/2008WR006848.
- Gleeson, T., L. Smith, N. Moosdorf, J. Hartmann, H. H. Durr, A. H. Manning, L. P. H. van Beek, and A. M. Jellinek (2011), Mapping permeability over the surface of the Earth, *Geophys. Res. Lett.*, 38, L02401, doi:10.1029/2010GL045565.
- Haitjema, H. M., and S. Mitchell-Bruker (2005), Are water tables a subdued replica of the topography?, *Ground Water*, 43(6), 781–786.
- Hay, L. E., S. L. Markstrom, and C. War-Garrison (2011), Watershed-scale response to climate change through the twenty-first century for selected basins across the United States, *Earth Interact.*, 15(17), 1–37.
- Huntley, D. (1979), Ground-water recharge to the aquifers of northern San Luis Valley, Colorado, *Geol. Soc. Am. Bull. Part 2*, 90(8), 1196–1281.
- Ingebritsen, S. E., and C. E. Manning (1999), Geologic implications of a permeability-depth curve for the continental crust, *Geology*, 27(12), 1107–1110.
- Jehn, J. (1997), *Percolation Test Report, South Park Conjunctive Use Project, Prepared for the City of Aurora, Jehn Water Consul., Inc.*, Denver, Colo.
- Jiang, X.-W., L. Wan, X.-S. Wang, S. Ge, and J. Liu (2009), Effect of exponential decay in hydraulic conductivity with depth on regional groundwater flow, *Geophys. Res. Lett.*, 36, L24402, doi:10.1029/2009GL041251.
- Johnson, J. B., and D. A. Stiengraaber (2003), The vegetation and ecological gradients of calcareous mires in the South Park valley, Colorado, *Can. J. Bot.*, 81(3), 201–219.
- Johnson, R. H. (2007), Ground water flow modeling with sensitivity analyses to guide field data collection in a mountain watershed, *Groundwater Monit. Rem.*, 27(1), 75–83.
- Keating, E. H., V. V. Vesselinov, E. Kwicklis, and Z. Lu (2003), Coupling basin and site scale inverse models of the Espanola Aquifer, *Groundwater*, 41(2), 200–211.
- Legg, T. M. (2011), *The Hydrology and Hydrochemistry of the High Creek Fen*, Univ. of Colo., Boulder, Colo.
- Lopez, D. L., and L. Smith (1995), Fluid flow in fault zones—Analysis of the interplay of convective circulation and topographically driven groundwater flow, *Water Resour. Res.*, 31(6), 1489–1503.
- Lopez, D. L., and L. Smith (1996), Fluid flow in fault zones: Influence of hydraulic anisotropy and heterogeneity on the fluid flow and heat transfer regime, *Water Resour. Res.*, 32(10), 3227–3235.
- Manning, A. H. (2011), Mountain-block recharge, present and past, in the eastern Espanola Basin, New Mexico, USA, *Hydrogeol. J.*, 19, 379–397.
- Manning, A. H., and D. K. Solomon (2005), An integrated environmental tracer approach to characterizing groundwater circulation in a mountain block, *Water Resour. Res.*, 41, W12412, doi:10.1029/2005WR004178.
- Marler, J., and S. Ge (2003), The permeability of the Elkhorn fault zone, South Park, Colorado, *Ground Water*, 41(3), 321–332.
- Pederson, G. T., J. L. Betancourt, and G. J. McCabe (2013), Regional patterns and proximal causes of the recent snowpack decline in the Rocky Mountains, U.S., *Geophys. Res. Lett.*, 40, 1811–1816, doi:10.1002/grl.50424.
- PRISM Climate Group (2006), *United States Average Monthly or Annual Precipitation, 1971–2000*, Oregon State Univ., Corvallis. [Available at <http://prism.oregonstate.edu>.]
- Robinson, C. S. (1978), Hydrology of fractured crystalline rocks, Henderson Mine, Colorado, *Mining Engineering*, 30, 1185–1194.
- Ruleman, C. A., R. G. Bohannon, B. Bryant, R. R. Shroba, and W. R. Premo (2011), Geologic map of the Bailey 30' × 60' quadrangle, north-central Colorado, *U.S. Geol. Surv. Sci. Invest. Map* 3156, 38 pp.
- Saar, M. O., and M. Manga (2004), Depth dependence of permeability in the Oregon Cascades inferred from hydrogeologic, thermal, seismic, and magmatic modeling constraints, *J. Geophys. Res.*, 109, B04204, doi:10.1029/2003JB002855.
- Sanford, W. E., L. N. Plummer, D. P. McAda, L. M. Bexfield, and S. K. Anderholm (2004), Hydrochemical tracers in the middle Rio Grande Basin, USA: 2. Calibration of a groundwater-flow model, *Hydrogeol. J.*, 12, 389–407.
- Scanlon, B. R., K. E. Keese, A. L. Flint, L. E. Flint, C. B. Gaye, W. M. Edmunds, and I. Simmers (2006), Global synthesis of groundwater recharge in semiarid and arid regions, *Hydrol. Processes*, 20, 3335–3370.
- Spahr, N. E. (1981), Variations in climatic characteristics as related to evapotranspiration in South Park, central Park County, Colorado, *U.S. Geol. Surv. Water Resour. Invest.*, 80–86, 162 pp.
- Sterne, E. J. (2006), Stacked, evolved triangle zones along the southeastern flank of the Colorado Front Range, *Mt. Geol.*, 43(1), 65–92.
- Susong D. D., L. E. Brooks, and J. L. Mason (1998), Water resources in the area of the Snyderville basin and Park City in Summit County, Utah, *U.S. Geol. Surv. Fact Sheet* 099–98, 4 pp.

- Tiedeman, C. R., D. J. Goode, and P. A. Hsieh (1998), Characterizing a ground water basin in a New England mountain and valley terrain, *Ground Water*, 36(4), 611–620.
- Topper, R., K. L. Spray, W. H. Bellis, J. L. Hamilton, and P. E. Barkmann (2003), Ground water atlas of Colorado, *Spec. Publ. 53*, Colo. Geol. Surv., Denver, Colo., 210 pp.
- Toth, J. (1963), A theoretical analysis of groundwater flow in small drainage basins, *J. Geophys. Res.*, 68(16), 4795–4812.
- Uchida, T., Y. Asano, N. Ohte, and T. Mizuyama (2003), Seepage area and rate of bedrock groundwater discharge at granitic unchanneled hillslope, *Water Resour. Res.*, 39(1), 1018, doi:10.1029/2002WR001298.
- Welch, L. A., and D. M. Allen (2012), Consistency of groundwater flow patterns in mountainous topography: Implications for valley bottom replenishment and for defining groundwater flow boundaries, *Water Resour. Res.*, 48, W05526, doi:10.1029/2011WR010901.
- Wilson, J. L., and H. Guan (2004), Mountain-block hydrology and mountain-front recharge, in *Groundwater Recharge in a Desert Environment: The Southwestern United States*, edited by F. M. Phillips, J. Hogan, and B. Scanlon, p. 23, AGU, Washington, D. C.
- Winter, T. C. (2001), The concept of hydrologic landscapes, *J. Am. Water Resour. Assoc.*, 37(2), 335–349.
- Zektser, S., H. A. Loaigiga, and J. T. Wolf (2005), Environmental impacts of groundwater overdraft: Selected case studies from the southwestern United States, *Environ. Geol.*, 47(3), 396–404.